Trans. of the Society of Instrument and Control Engineers
Vol. E-1, No.1, 305/311 (2001)

Emissivity Compensated Radiation Thermometry Using Directional Radiance†

Tohru IUCHI* , Tomoyuki TSURUKAWAYA** and Akira TAZOE***

Emissivity of a metal is fairy low in its bare condition. Due to oxide films formed on the metal surface, however, its emissivity changes rapidly, and large errors in the temperature measurement are caused. This is a serious problem for the radiation thermometry of metals. In order to eliminate the error due to surface conditions of the objects, the authors propose a new method based on their findings that the apparent emissivity of a metal surface depends on the direction from which the target is looked at. This means that the radiance of the target does not obey Lambert law. The proposed method uses the ratio of radiances measured at two different angles to compensate the emissivity or the emissivity ratio. This method is promissing for the in-line use at metal manufacturing processes such as steels and aluminums and so on.

Key Words : radiation thermometry. emissivity. metal. oxide film. radiance.

1. Introduction

The emissivity change is a serious problem in radiation thermometry, because it causes the temperature error to a large extent. Therefore, radiation thermometry for solving the emissivity problem has been studied from various view points. These methods, that is to say, emissivity compensated radiation thermometry roughly is divided into two techniques. The one is called an active method or a hybrid method that estimates the emissivity of the object or minimizes the effect of the emissivity using reciprocal process of radiation between the object and a reflector that is introduced in a measurement system [1,2]. The other is a passive method that is often called a multiband radiometer that estimates the temperature of the object using detected spectral radiances more than two [3-5].

This paper describes a new method that measures an emissivity of a metal using directional properties of spectral radiances emitted from the object that in turn enables to obtain the temperature of the metal. Accordingly, this method is a passive one [6-8]. The normal emissivity of a metal is quite low generally, but it increases gradually with increasing angle measured from the normal of the surface, and it attains its maximum value at nearly 80˚, and then decreases rapidly to zero at an angle of 90˚. The emissivity of the metal covered with the oxide film on its surface, on the other hand, is high generally, but monotonically decreases with increasing angle. These properties of emissivity correspond to the optical constants of a metal as a conductor and oxide film as dielectrics, respectively, which are led from Maxwell's electromagnetic equations [9]. These phenomena show that the radiances of these materials do not obey the Lambert law. Considering these phenomena, the ratio of radiances at two different angles, for example, at 20˚ and 80˚, strongly depends on the surface conditions of the metal on which oxide film is grown, therefore the ratio assumes to be an excellent figure to estimate the spectral emissivity of the metal.

Based on the above phenomena, the authors have proposed an emissivity-compensated radiation thermometry.

2. Theoretical

The Fresnel formulas, which can be derived from Maxwell's equations, are expressions for the reflectivity of an ideally smooth and optically homogeneous plane surface to incident electromagnetic radiation, in terms of the optical constants, n and k of the surface meterial and θ, the angles of incidence and reflection. From these formulas, with the aid of Kirchhoff's law, the magnitude and the directional distribution of the emissivity can be inferred [10]. The spectral emissivity $\varepsilon_\lambda(\theta)$ at a wavelength of λ and a direction of θ is shown as follows,

$$\varepsilon_\lambda(\theta) = \frac{1}{2}\,\varepsilon_{\lambda,s}(\theta)\,[\,1+ \frac{a^2 + b^2 + \sin^2\theta}{\cos^2\theta\,(\,a^2 + b^2 + 2a\sin\theta\tan\theta + \sin^2\theta\tan^2\theta\,)}\,] \tag{1}$$

$$\varepsilon_{\lambda,s}(\theta) = \frac{4a\cos\theta}{a^2 + b^2 + 2a\cos\theta + \cos^2\theta} \tag{2}$$

where $\varepsilon_{\lambda,s}(\theta)$ is a directional emissivity that is polarized perpendicular to the plane of incidence.

The quantities a and b are related to the angle of θ and to the refractive index n and the extinction coefficient k of the material on which the radiation is incident.

$$2a^2 = \sqrt{(n^2 - k^2 - \sin^2\theta)^2 + 4n^2k^2} + (n^2 - k^2 - \sin^2\theta) \tag{3}$$

$$2b^2 = \sqrt{(n^2 - k^2 - \sin^2\theta)^2 + 4n^2k^2} - (n^2 - k^2 - \sin^2\theta) \tag{4}$$

† Partially presented at SICE' 95

* Department of Mechanical Engineering, Toyo University, Kawagoe
** Mitutoyo Co., Kawasaki,
*** Toyo University, now SPC Electronics Corp., Chofu, Tokyo
** now, Kyoritsu Seiki Ltd. Tokyo

If the optical constants of the material n and k are known, Eq.(1) provides a prediction of the directional disribution of the spectral emissivity of the material. The parameter θ is the angle of emission in the present context. Generally, with increasing value of k, the material shows electrically conductive, and with decreasing value of k, on the other hand, it becomes electrically nonconductive. Fig.1(a) shows the predicted directional distribution of the emissivity which changes with the optical constants.

where $L_{\lambda,b}(T)$ is the spectral blackbody radiance of the temperature T at λ. Let R_e be the ratio of the above radiances $L_\lambda(\theta_2)$ and $L_\lambda(\theta_1)$, then it becomes the ratio of the emissivities at two directions, θ_2 and θ_1 as shown below,

$$R_e = L_\lambda(\theta_2) / L_\lambda(\theta_1) = \varepsilon_\lambda(\theta_2) / \varepsilon_\lambda(\theta_1) \tag{7}$$

The spectral emissivity ε_λ of a metal at any angle θ is expected to increase with growing oxide film on its surface as shown in Fig.2.

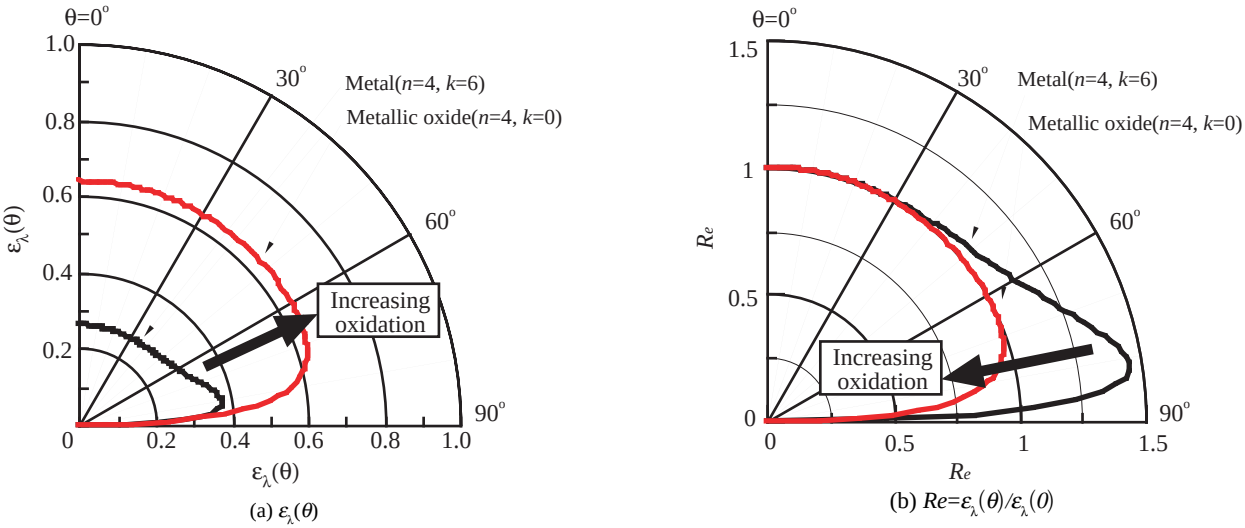

Fig.1 Directional emissivity

For an electric nonconductor (k=0), the emissivity appears to be essentially uniform over the range of angles between 0˚ and about 60˚, then it drops sharply to zero. With increasing values of k, the directional emissivity displays a maximum at a moderately large value of θ, for example, at 80˚, and then returns to zero at θ=90˚. Fig.1(b) shows the normalized figure $R_e=\varepsilon_\lambda(\theta)/\varepsilon_\lambda(0)$ that represents well the above description of the phenomena concerning to an electric conductor and an electric nonconductor.

Though the surface of a commercial base metal such as a cold rolled steel sheet is not optically smooth in the strict sense of the word, it is assumed that the surface condition of the metal before oxidation keeps the features of the electric conductor concerning to the emissivity. When the metal is heated in air, however, its surface becomes nonconductive because of the oxide film covered on it. Therefore, the figure R_e changes drastically near 80˚ with growing oxide film.

Now, let $L_\lambda(\theta_1)$ and $L_\lambda(\theta_2)$ be the spectral radiances of the object of the temperature T at λ and at directions θ_1 and θ_2 ($\theta_1<\theta_2$), respectively,

$$L_\lambda(\theta_1) = \varepsilon_\lambda(\theta_1)\cdot L_{\lambda,b}(T) \tag{5}$$

$$L_\lambda(\theta_2) = \varepsilon_\lambda(\theta_2)\cdot L_{\lambda,b}(T) \tag{6}$$

Accordingly, a relation between R_e and ε_λ is presumed to hold as shown in Fig.4(a) from the characteristics of Figs.1 and 2. Moreover, as the ratio $\varepsilon_R = \varepsilon_{\lambda1}(\theta) / \varepsilon_{\lambda2}(\theta)$ of spectral emissivities at two wavelengths λ_1 and λ_2 ($\lambda_1 < \lambda_2$) is estimated to decrease with increasing oxidation, a relation between R_e and ε_R also is presumed to hold as shown in Fig.4(b).

If the relation of Fig.4(a) is constructed once, a spectral emissivity $\varepsilon_\lambda(\theta)$ can be obtained by using the measurement of the ratio R_e. Thus, a true temperature T of the object can be derived from substituting the obtained $\varepsilon_\lambda(\theta)$ into Eq.(5) or Eq.(6). This method is named as ε_λ-compensated radiation thermometry from now. Likewise, the measurement of R_e provides the ratio ε_R as shown in Fig.4(b). A true temperature T is obtained by substituting this ε_R into the well-known formula of two color pyrometry in Eq.(8) [6]. This method ia called as ε_R-compensated radiation thermometry from now.

$$R = \frac{L_{\lambda1}(\theta)}{L_{\lambda2}(\theta)} = \varepsilon_R \left(\frac{\lambda_2}{\lambda_1}\right)^5 \exp\left(-\frac{c_2}{\Lambda T}\right) \tag{8}$$

where $\Lambda=\lambda_1\lambda_2/(\lambda_2-\lambda_1)$ and c_2=Planck's second constant.

R_e is a non-dimensional figure that represents the change of the directional properties of emissivity depending on the variation of a metal surface during the oxidizing process. Therefore, R_e is a potential figure that can be used for a measurement of the behavior

of the oxide film on the metal surface as well as an application to radiation thermometry.

large change of emissivity. A sample with 88 mm in diameter and 1 mm in thickness was used.

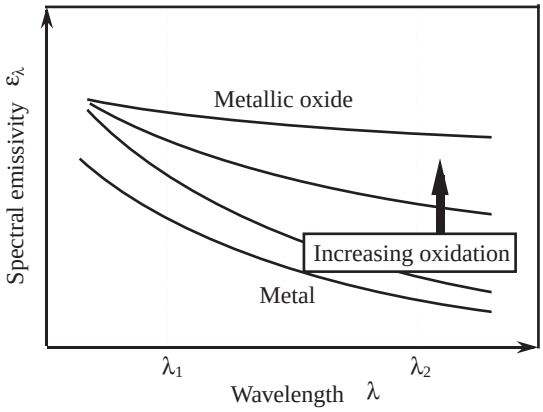

Fig.2 Change of ε_λ with increasing oxidation

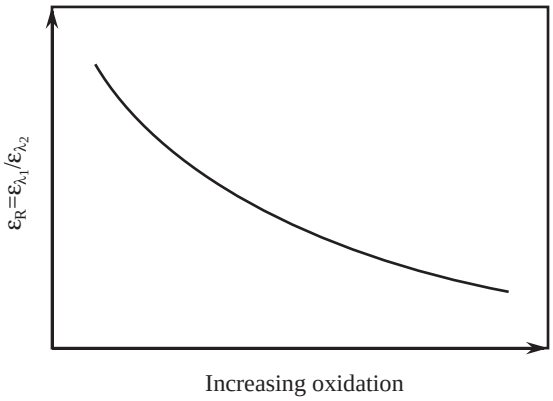

Fig.3 Change of ε_R with increasing oxidation

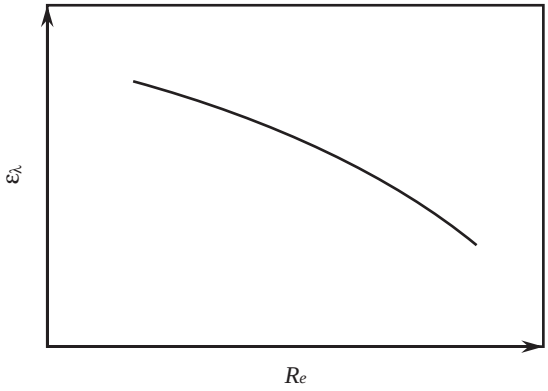

(a) *Re* and ε_λ

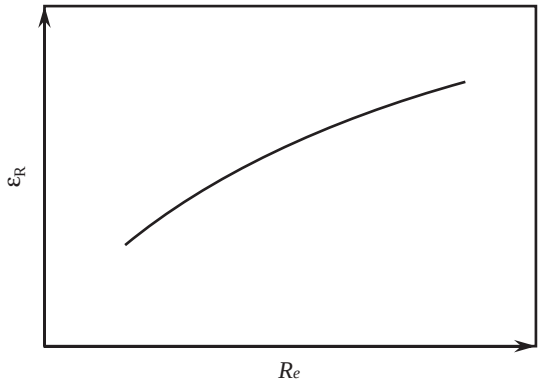

(b) *Re* and ε_R

Fig.4 Predicted relations (a) between *Re* and ε_λ, (b) between *Re* and ε_R

3. Experimental

Fig.5 shows an experimental apparatus that has been used for the confirmation of the measurement principle. In order to measure radiances, three radiometers were used. The two of them were set at a direction of θ_1=20˚ to measure the ratio ε_R of spectral emissivities at two wavelengths λ_1 and λ_2. A semiconductor InGaAs sensor effective at λ_1 =1.5 μm and a pyroelectric $LiTaO_3$ effective at λ_2=3.4 μm, were used for these radiometers, respectively. The third radiometer with a pyroelectric sensor, $LiTaO_3$ effective at λ_2=3.4 μm was set at a direction of θ_2=80˚. The ratio $R_e = L_{\lambda 2}(\theta_2) / L_{\lambda 2}(\theta_1)$ was calculated by using the radiances $L_{\lambda 2}(\theta_2)$ and $L_{\lambda 2}(\theta_1)$ that were measured by the latter two radiometers at θ_2=80˚ and θ_1=20˚, respectively. The ratio $\varepsilon_R = \varepsilon_{\lambda 1}(\theta_1) / \varepsilon_{\lambda 2}(\theta_1)$ at θ_1=20˚ was derived from the measurements of the former two radiometers. True temperature of a specimen surface was obtained by a K-type thermocouple welded on the surface of the object. Cold rolled steel sheets were selected as metal specimens that were easy to oxidize at rather low temperatures of about 700 K, thus enabling to cause

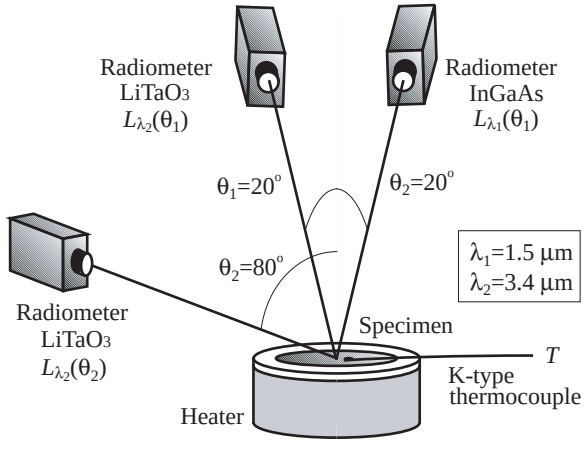

Fig.5 Experimental apparatus

According to a preparaory experiment, the temperature distribution on the specimen surface was about ±5 K within 30 mm from the center of the sample. In order to estimate the measurement error of temperature by a thermocouple, the black paint that was

assumed to be a pseudo-blackbody (effective emissivity is about 0.92) was applied to the surface of a specimen, then the temperature of the surface was measured by a radiometer with a InGaAs sensor. The temperature by measurement of the latter was regarded as the true temperature of the specimen surface. The difference between the true temperature and the temperature measured by the thermocouple was about 7 K near 800 K. As the temperature error by the measurement of a thermocouple and the temperature distribution on the surface of a specimen were assumed to be systematic errors, the reproducibility of the measurement was kept by welding a thermocouple to a specified position of the sample. The detected area by a radiometer was 5 mm in diameter when it was looked from the normal direction, but it became an ellipse when looked from a direction of θ_2=80˚. The length at the major axis was about 28 mm. The sample had enough size to cover detected area on the sample when the sample was looked at θ_2=80˚.

Fig.6 showed the changes of directional emissivities , $\varepsilon_{\lambda 2}(\theta_1)$ and $\varepsilon_{\lambda 2}(\theta_2)$, at a wavelength λ_2 =3.4 μm, and their ratio $R_e = \varepsilon_{\lambda 2}(\theta_2) / \varepsilon_{\lambda 2}(\theta_1)$ of a specimen during heating in air to 723 K. In the early stage of heating, the emissivity at θ_2=80˚ was higher than the emissivity at θ_1=20˚, thus the ratio R_e in Eq.(7) displayed a high value. The directional emissivities, however, rapidly changed with increasing time, that is, the emissivity at θ_1=20˚ became higher than the emissivity at θ_2=80˚. Accordingly, R_e decreased drastically from a higher value to a lower value. These results corresponded with the prediction of a measurement principle as shown in Fig.4(a).

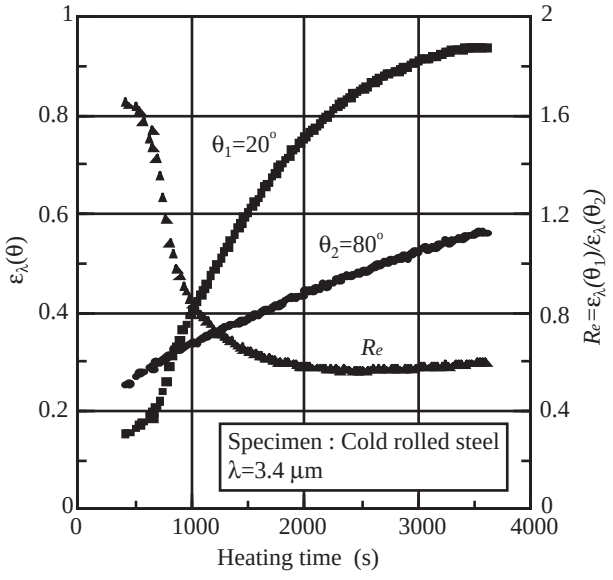

Fig.6 Experimental results of $\varepsilon_{\lambda 1}(\theta_1)$ and $\varepsilon_{\lambda 2}(\theta_2)$ at λ_2 =3.4 μm and the ratio $R_e = \varepsilon_{\lambda 2}(\theta_2) / \varepsilon_{\lambda 2}(\theta_1)$

Fig.7 likewise showed the variations of the directional spectral emissivities $\varepsilon_{\lambda 1}(\theta_1)$ and $\varepsilon_{\lambda 2}(\theta_1)$ at a direction of θ_1=20˚, and their ratio $\varepsilon_R = \varepsilon_{\lambda 1}(\theta_1) / \varepsilon_{\lambda 2}(\theta_1)$ of a specimen during heating in air to 723 K. In the early stage of heating, both the emissivities $\varepsilon_{\lambda 1}(\theta_1)$ and $\varepsilon_{\lambda 2}(\theta_1)$ increased rapidly. The emissivity $\varepsilon_{\lambda 1}(\theta_1)$ at a shorter wavelength of λ_1 =1.5 μm, however, took a peak value, then decreased. The emissivity $\varepsilon_{\lambda 2}(\theta_1)$ at a longer wavelength of λ_2 =3.4 μm, on the other hand, continued to increase. As a result, the ratio ε_R raised in the early stage of heating and had a peak value, then decreased. Because of the difference between these phenomena and a predicted relation of Fig.3, considerations on this cause have been done in section 4.

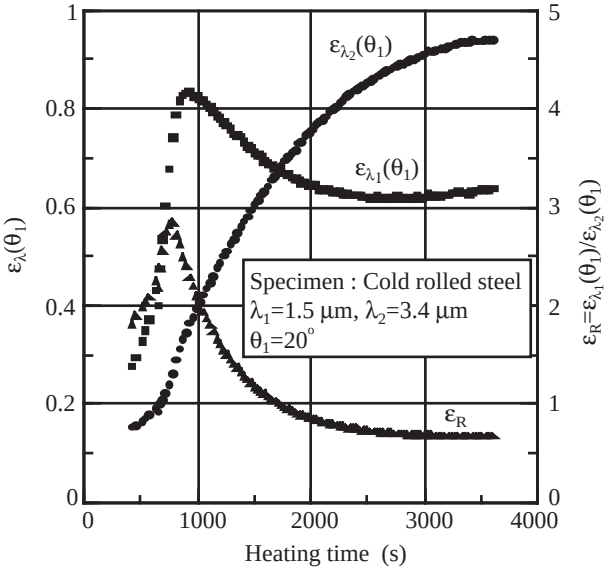

Fig.7 Experimental results of $\varepsilon_{\lambda 1}(\theta_1)$ and $\varepsilon_{\lambda 2}(\theta_1)$ at θ_1=20˚ and the ratio $\varepsilon_R = \varepsilon_{\lambda 1}(\theta_1) / \varepsilon_{\lambda 2}(\theta_1)$

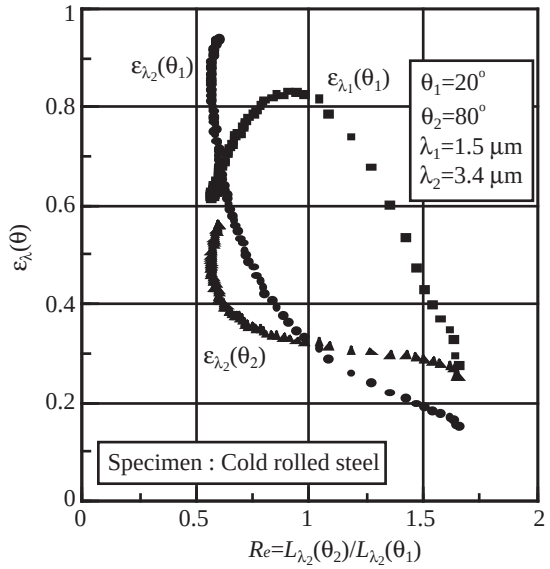

Fig. 8 Experimental relation between *Re* and $\varepsilon_\lambda(\theta)$

Fig.8 displayed the characteristic curves between R_e and $\varepsilon_\lambda(\theta)$ that were derived from Figs.6 and 7. In this figure, the changes of three emissivities, $\varepsilon_{\lambda 1}(\theta_1)$, $\varepsilon_{\lambda 2}(\theta_1)$ at θ_1=20˚, and $\varepsilon_{\lambda 2}(\theta_2)$ at θ_2=80˚ were

plotted for the change of R_e that corresponded with a predicted relation of Fig.4(a). These relations proved that the ε_λ-compensated radiation thermometry is valid, that means if R_e is derived from the measurement of directional, spectral radiances at two different angles, the emissivity $\varepsilon_\lambda(\theta)$ is uniquely obtained, then the temperature of a specimen can be calculated. Fig.9 likewise showed the characteristic curve between R_e and ε_R that were also derived from Figs.6 and 7. From the measurement of R_e, the emissivity ratio ε_R used for two color pyrometry can be obtained, thus it enables to calculate the true temperature of a specimen. This is the ε_R-compensated radiation thermometry.

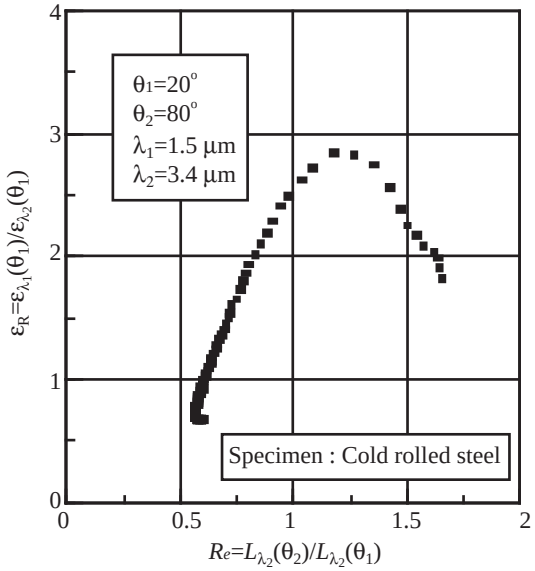

Fig.9 Experimental relation between *Re* and ε_R

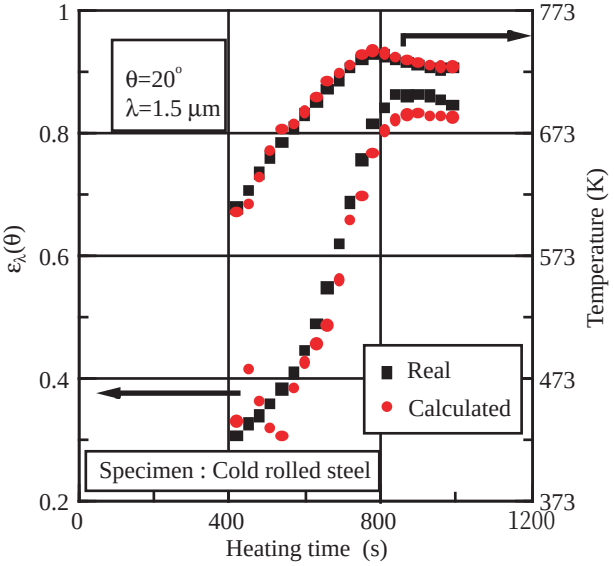

Fig.10 Online measurement of $\varepsilon_\lambda(\theta)$ and T

Fig.10 showed an experimental result of simultaneous measuremet of temperature T and emissivity $\varepsilon_\lambda(\theta)$ which was based on the ralation of Fig.8, where spectral emissivity at λ =1.5 μm and at θ =20° was obtained. In this figure, real temperatures measured by a K-type thermocouple and real emissivities that were obtained using the real temperatures, and calculated temperatures and calculated emissivities that were derived from the ε_λ-compensated radiation thermometry were plotted simultaneously. In spite of large changes of the emissivities, it was observed that the calculated temperatures well corresponded with the real ones. Similarly, Fig.11 displayed an experimental result of simultaneous measurement of temperature T and emissivity ratio ε_R which was based on the relation of Fig.9, where spectral emissivity ratio $\varepsilon_R = \varepsilon_{\lambda1}(\theta_1) / \varepsilon_{\lambda2}(\theta_1)$ at λ_1 =1.5 μm and λ_2 =3.4 μm, and θ_1=20° was obtained. The calculated temperatures that were based on the ε_R-compensated radiation thermometry and the real temperatures that were derived from a K-type thermocouple well corresponded, though ε_R changed largely.

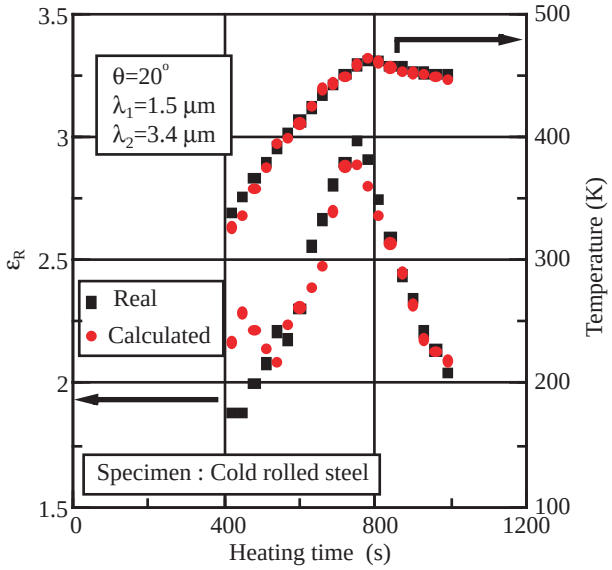

Fig.11 Online measurement of ε_R and T

4. Considerations

It is assumed that oscillating changes of the spectral emissivity $\varepsilon_{\lambda1}(\theta_1)$ at λ_1 =1.5 μm and at θ_1=20° and the ratio ε_R during heating are caused by the interference effect of radiation between the sample surface and the oxide film grown on it [11]. That means, both of the spectral emissivities $\varepsilon_{\lambda1}(\theta_1)$ and $\varepsilon_{\lambda2}(\theta_1)$ increase with increasing thickness of the oxide film at the early stage during heating. But in the mean time, the emissivity $\varepsilon_{\lambda1}(\theta_1)$ at a shorter wavelength of λ_1 =1.5 μm has its peak value due to the interference effect, then decreases, while the emissivity $\varepsilon_{\lambda2}(\theta_1)$ at a longer wavelength of λ_2 =3.4 μm still increases. This phenomon causes the occurence of a peak value for the ratio ε_R. As there is one by one correspondence between R_e and ε_R in Fig.9, the principle of measurement based on the theory holds.

The ratio R_e decreases with increasing oxidation and it finally converges to about 0.55 as shown in Fig.6. At this value, spectral emissivities $\varepsilon_{\lambda1}(\theta_1)$ and $\varepsilon_{\lambda2}(\theta_1)$ and emissivity ratio

Table 1 Measurement errors by the method for bright and dull surfaces of cold rolled steel sheets (T=800 K)

	Wavelength λ (μm)	Specimen type	Emissivity ε_λ	Emissivity error $\lvert\Delta\varepsilon/\varepsilon\rvert_{max}$	Temperature error $\lvert\Delta T/T\rvert_{max}$
ε_λ-compensated method	λ_1=1.5 μm	dull	0.28~0.86	0.065	0.005
		bright	0.25~0.94	0.010	0.008
	λ_2=3.4 μm	dull	0.15~0.96	0.093	0.016
		bright	0.14~0.97	0.080	0.014
	Wavelength λ (μm)	Specimen type	Emissivity ε_λ	Emissivity ratio error $\lvert\Delta\varepsilon_R/\varepsilon_R\rvert_{max}$	Temperature error $\lvert\Delta T/T\rvert_{max}$
ε_R-compensated method	λ_1=1.5 μm λ_2=3.4 μm	dull	3.0~0.7	0.056	0.008
		bright	2.9~0.8	0.081	0.012

$\varepsilon_R = \varepsilon_{\lambda1}(\theta_1) / \varepsilon_{\lambda2}(\theta_1)$ vary one another. These phenomena should also be caused by the interference of radiation between the bare metal surface and the oxide film. As the emissivities are high and the change of ε_R is small generally at R_e=0.55, the measurement error of temperature remains to be small. As the interference phenomena, however, is not preferable for the principle of this method, a new procedure to negate this phenomena is necessary. The one of powerful methods for that is to utilize a radiometer that responds to longer wavelengths as expected from the behavior of two emissivities $\varepsilon_{\lambda1}(\theta)$, $\varepsilon_{\lambda2}(\theta)$ in Fig.7. The detailed discussions and the development of the procedure are to be reported [12].

Table 1 shows the measurement errors of temperature and emissivity by the method for bright and dull surfaces of cold rolled steel sheets. The experiments were done at 800 K. There was a slight difference between the characteristic curves for bright and dull surfaces caused by the difference of surface roughness, thus the errors were arranged separately in Table 1. In case of dull surfaces, for example, the spectral emissivity $\varepsilon_\lambda(\theta)$ at λ =1.5 μm and θ=20˚ changed from 0.28 to 0.86, the relative errors $|\Delta\varepsilon/\varepsilon|$ and $|\Delta T/T|$ of emissivity and temperature calculated by the principle of the ε_λ-compensated radiation thermometry, however, were 0.065 and 0.005, respectively. Likewise, the emissivity ratio ε_R at λ =1.5 μm and λ =3.4 μm changed from 3.0 to 0.7, the relative error $|\Delta\varepsilon_R/\varepsilon_R|$ and $|\Delta T/T|$ of emissivity ratio and temperature calculated by the principle of the ε_R-compensated radiation thermometry, however, were 0.056 and 0.008, respectively. In Table 1, the relative error of emissivity $|\Delta\varepsilon/\varepsilon|$ was obtained by using the characteristic curve between R_e and ε_λ in Fig.8, where $\Delta\varepsilon$ was the difference between the emissivity that was derived from the measurement of R_e and the true emissivity that was obtained by the temperature measured by a K-type thermocouple, that in turn was used to calculate the emissivity of a specimen. The denominator was the emissivity of the latter. The relative error of emissivity ratio $|\Delta\varepsilon_R/\varepsilon_R|$ was derived from Fig.9 in a similar procedure as stated above. The temperature difference ΔT in the relative error of temperature $|\Delta T/T|$ was obtained as the difference between the true temperature T measured by a K-type thermocouple and the temperature measured by the principle of the method. The denominator was the true temperature measured by the thermocouple.

According to the experimental results, the ε_R-compensated radiation thermometry practically got similar accuracy in measurement as the ε_λ-compensated radiation thermometry. The signal processing for the former as conventional two color pyrometry, however, was rather complicated than the latter, so that the ε_λ-compensated radiation thermometry should be preferable for a practical use.

5. Conclusion

The authors proposed the ε_λ-compensated radiation thermometry and the ε_R-compensated radiation thermometry that compensate an emissivity or an emissivity ratio, respectively, by using a ratio R_e of two spectral radiances that are measured from two different directions. These methods are experimentally confirmed to be promising for online temperature measurements of metals during oxidizing process. In order to improve resolution of these methods, the one of the radiometers is preferable to be set at a direction between the normal and 60˚, especially between the normal and 30˚. The other of the radiometers should be set at a direction between 60˚ and 85˚, but judging from practical view point, a direction between 70˚ and 80˚ is preferable.

Emissivities of metals change due to the interference effect with the growth of oxide film on their surfaces. It is necessary for wide applications of these methods to find a procedure to avoid the

interference effect. The usage of a longer wavelength for the measurement of R_e is one method to ease the interference effect [12]. Cold rolled steel sheets are mostly used for experiments. Other metals that represent much more clearer interference effect, however, may be much better objects for these methods.

The authors have confirmed that a usage of polarization instead of directional properties of radiances is possible for emissivity compensated pyrometry, and also the combination of directional and polarized properties of a metal is promising for wide applications of radiation thermometry [13,14]. There are some fundamental problems left to be investigated. That is, the influence of variations of surface roughness and compositions of materials to a characteristic curve of the method should be considered and an effective procedure to ease the influence should be developed. A compact measurement system using fibers is under consideration for a practical use of the principle.

Acknowledgement

This research is partly funded by the Ministry of Education, Science, Sports and Culture under Grand-in-Aid for Scientific Research (C) (Project Number 10650416. fiscal year 1995) and in part by KAWASAKI STEEL 21st Century Foundation (fiscal year 1995).

References

1) T. Iuchi and R. Kusaka: Two methods for simulaneous measurement of temperature and emittance by using multiple reflection and specular reflection, and their applications to industrial processes, TEMPERATURE, **5**, 491/503 (1982)
2) T. Iuchi: Applications of RADIATION THERMOMETRY, (edited y J.C. Richmond and D.P. DeWitt), ASTM STP 895, 121/150 (1986)
3) M.A. Pellerin, B.K. Tsai, D.P. DeWitt and G.D. Dail: Emissivity compensated methods for aluminum alloy temperature determination, TEMPERATURE, **6**, 871/876 (1992)
4) F. Tanaka and H. Ohira: Thermometry restablished by automatic compensation of emissivity; The TRACE method, TEMPERATURE, **6**, 895/900 (1992)
5) D.Y. Svet: Some new methods and systems of pyrometry and their application, TEMPERATURE, **4**, 587/597 (1972)
6) T. Tsurukawaya and T. Iuchi: New ratio pyrometry compensating change of emissivity ratio, Proc. of the 12th SENSING FORUM, 79/84 (1995)
7) T. Tsurukawaya, T. Nakadai and T. Iuchi: New radiation thermometry using directional emissivity, Proc. of the 34th SICE Annual Conference, 212A-3, 647/648 (1995)
8) T. Iuchi and T. Tsurukawaya: New radiation thermometry using directional emissivity, Proc. of TEMPMEKO' 96, Torino, 359/364 (1996)
9) R. Siegel and J.R. Howell: Thermal radiation heat transfer, 82, McGraw-Hill, (1972)
10) E.M. Sparrow and R.D. Cess: Radiation heat transfer, 64, Hemisphere, (1978)
11) G. Neuer: On the influence of radiation properties when measuring temperatures of oxidized metals and ceramics, Practical Surface Pyrometry Workshop, Delft, Topic-6, 1/12 (1993)
12) T. Iuchi, T. Hoshino, T. Furukawa and A. Tazoe: Polarization characteristics of metals during oxidating process and its application to emissivity-compensated radiation thermometry, Trans. of SICE, **35**-7, 832/839 (1999)
13) T. Tsurukawaya, T. Furukawa and T. Iuchi: Emissivity compensated radiation thermometry, Proc. of the 35th SICE Annual Conference, 111A-5, 319/320 (1996)
14) T. Iuchi, T. Furukawa and T. Tsurukawaya: Measurement of polarization properties of metals and their applications to radiation thermometry, Proc. of the 14th IMEKO, Tampere, **6**, 108/113 (1997)

Tohru IUCHI (Member)

He received B.E. from Kyushu Institute of Technology in 1966, and M.S. and Ph.D. from Tokyo Institute of Technology in 1968 and 1980, respectively. He had been Nippon Steel Corp. from 1968 to 1991. He has been a professor at Toyo University, Department of Mechanical Engineering since 1991. He is a member of Japan Society of Applied Physics, Optical Society of America, International Society for Optical Engineering and so on .

Tomoyuki TSURUKAWAYA (Member)

He received B.E. and M.S. from Toyo University in 1993 and 1995, respectively. He joined Mitutoyo Co. in 1995. He is currently in Kyoritsu Seiki Corp. He is a member of the Japan Society of Mechanical Engineers. His current interests are designing and manufacturing of precision machines.

Akira TAZOE (Member)

He received B.E. and M.S. from Toyo University in 1994 and 1996, respectively. He has been in SPC Electronics Corp. since 1996. His main works are designs of IT instruments such as cellular phones.

Reprinted from Trans. of the SICE, Vol.34, No.3, 175/181 (1998)